Charge Trapping-Based Electricity Generator (CTEG): An Ultrarobust and High Efficiency Nanogenerator for Energy Harvesting from Water Droplets

Hao Wu,* Niels Mendel, Stijn van der Ham, Lingling Shui, Guofu Zhou,* and Frieder Mugele*

Strategies toward harvesting energy from water movements are proposed in recent years. Reverse electrowetting allows high efficiency energy generation, but requires external electric field. Triboelectric nanogenerators, as passive energy harvesting devices, are limited by the unstable and low density of tribo-charges. Here, a charge trapping-based electricity generator (CTEG) is proposed for passive energy harvesting from water droplets with high efficiency. The hydrophobic fluoropolymer films utilized in CTEG are pre-charged by a homogeneous electrowetting-assisted charge injection (h-EWCI) method, allowing an ultrahigh negative charge density of 1.8 mC m^{-2}. By utilizing a dedicated designed circuit to connect the bottom electrode and top electrode of a Pt wire, instantaneous currents beyond 2 mA, power density above 160 W m^{-2}, and energy harvesting efficiency over 11% are achieved from continuously falling water droplets. CTEG devices show excellent robustness for energy harvesting from water drops, without appreciable degradation for intermittent testing during 100 days. These results exceed previously reported values by far. The approach is not only applicable for energy harvesting from water droplets or wave-like oscillatory fluid motion, but also opens up avenues toward other applications requiring passive electric responses, such as diverse sensors and wearable devices.

Due to the increasing threat of energy crisis and global warming, searching and utilizing new energy resources become urgent and challenging. Natural water motions are clean and renewable energy resources, existing ubiquitously on the earth. Strategies have been proposed toward harvesting energy from water movements, such as reverse electrowetting,[1,2] triboelectric nanogenerators[3–8] and droplet-based electricity generator (DEG).[9] However, inherent flaws exist in current approaches. Reverse electrowetting energy harvesting devices always need external voltages.[1] Triboelectric nanogenerator (TENG),[10,11] which was first invented in 2012 by Wang and coworkers,[12,13] has provided a passive energy harvesting approach. But the performance of TENG is limited by the low density and poor stability of surface charges on tribo-layers. High surface charge density could only be achieved in vacuum environment[14] or by utilizing external pumping or excitation sources.[11,15] The droplet energy harvesting efficiency of the conventional TENG was only 0.01%.[5] Recently, Z. K. Wang and coworkers have reported a water drop-based electric generator, DEG,[9] showing significantly enhanced energy harvesting efficiency to 2.2%. Nevertheless, the energy harvesting efficiency of DEG is still limited by the density and stability of charges generated by triboelectrification during drop impact. The maximum surface charge density of DEG displayed around 0.184 mC m^{-2} (49.8 nC for 2.7 cm^2).[9] The surface charges in DEG were superior stability compared to the conventional TENG, although the charge density still degraded in a harsh environment with 100% humidity. Moreover, the efficiency greatly dropped with increasing salt

Dr. H. Wu, Prof. G. Zhou
Guangdong Provincial Key Laboratory of Optical Information Materials and Technology & Institute of Electronic Paper Displays
South China Academy of Advanced Optoelectronics
South China Normal University
Guangzhou 510006, P. R. China
E-mail: haowu@m.scnu.edu.cn; guofu.zhou@m.scnu.edu.cn

The ORCID identification number(s) for the author(s) of this article can be found under https://doi.org/10.1002/adma.202001699.

Dr. H. Wu, Prof. L. Shui, Prof. G. Zhou
National Center for International Research on Green Optoelectronics
South China Normal University
Guangzhou 510006, P. R. China

Dr. H. Wu, N. Mendel, S. van der Ham, Prof. F. Mugele
Physics of Complex Fluids
Faculty of Science and Technology
MESA+ Institute for Nanotechnology
University of Twente
Enschede 7500AE, The Netherlands
E-mail: f.mugele@utwente.nl

Prof. G. Zhou
Academy of Shenzhen Guohua Optoelectronics
Shenzhen 518110, P. R. China

concentration. The challenges are still remained in searching for an approach to achieve robust and high efficiency nanogenerators toward water-related applications.

Here, we report a strategy to achieve this goal, a Charge Trapping based Electricity Generator (CTEG), which presents a high energy conversion efficiency over 11% and excellent robustness during 100 days of intermittent testing without appreciable degradation. This CTEG relies on a dedicated substrate design and charging method[16] that is based on the recently discovered Electrowetting-assisted Charge Injection (EWCI) phenomenon.[17] The advantage of EWCI is that the trapped charges are highly stable and the density of negative charges does not degrade even in water vapor environment.[17] Thanks to our recently proposed electrical current design with a Pt wire in direct contact with the drop,[18] the electric current can be generated between the two electrodes. In a previous report, charge densities up to 0.46 mC m^{-2} have been achieved utilizing the EWCI method. However, these charge densities were highly localized and could not be increased any further due to the finite dielectric strength of fluoropolymer (FP) coatings (20–200 V μm^{-1} depending on the preparation process[19–22]) in combination with diverging electric fields at the air-water-solid contact. In this work, we therefore develop a new homogeneous electrowetting-assisted charge injection (h-EWCI) method by introducing a SiO$_2$ layer with much higher electric strength[23] than the polymer layer in combination with a mask to suppress the well-known divergence of the electric fields[17,24] and local dielectric breakdown near the contact line. As a result, a high electric field can be applied uniformly on a large area of dielectric stacks. Thus, a homogeneous maximum charge density of 1.8 mC m^{-2} has been achieved across a cm^2 large area of the FP surface. Distinct from the TENGs and the DEGs, this proposed CTEG does not rely on contact electrification upon drop impact on the solid surface. Thereby it overcomes the disadvantages of

instability and unpredictability of surface charges generated on the tribo-layers.

Figure 1a,b illustrate the proposed h-EWCI method for generating surface charges. A doped-Si wafer serves as the bottom electrode, and a thermally grown SiO$_2$ layer serves as the dielectric layer. A fluoropolymer (FP) film is spin coated on top of the SiO$_2$ surface in a cleanroom and a mask of polypropylene (PP) tapes is applied to define the surface area, typically a field of 1 cm^2, that is to be charged. A big puddle of water (several milliliters) is placed on top of the FP surface covering the entire surface including the PP masks to suppress the formation of a free and mobile air-water-solid three phase contact line. Subsequently, a charging voltage U_c up to −400 V (relative to the grounded bottom electrode) is applied across the dielectric layers via the water puddle for 15 min. After that, the voltage and the water are removed. Throughout the charging process, the current density does not exceed 0.2 μA cm^{-2}, such that the total electrical energy input during charging is less than 0.02 J cm^{-2} (Figure S1, Supporting Information). Note that this charging procedure is applied only once upon fabrication of the substrate and does not need to be renewed neither during continuous nor during intermittent operation. Like conventional EWCI,[17] the h-EWCI charging process does not affect the topography of the FP surface, see Figure 1c. In contrast to EWCI, however, the surface charge density in h-EWCI is now homogeneous across the entire charging area, which is essential for CTEG. Figure 1d shows the surface charge density detected by an electrowetting probe. When there is no charge on the surface, the EW curve is symmetrical with $U = 0$ V. Once there are charges existing on the hydrophobic surfaces, the symmetry axis shifts from $U = 0$ V to $U = U_T$, and the surface charge density σ_T could be calculated by $\sigma_T = U_T c$, where c is the capacitance per area of the dielectric layer.[17,25] Given all the surface charges are negative in this work, we define σ as the absolute value of the σ_T. σ as high
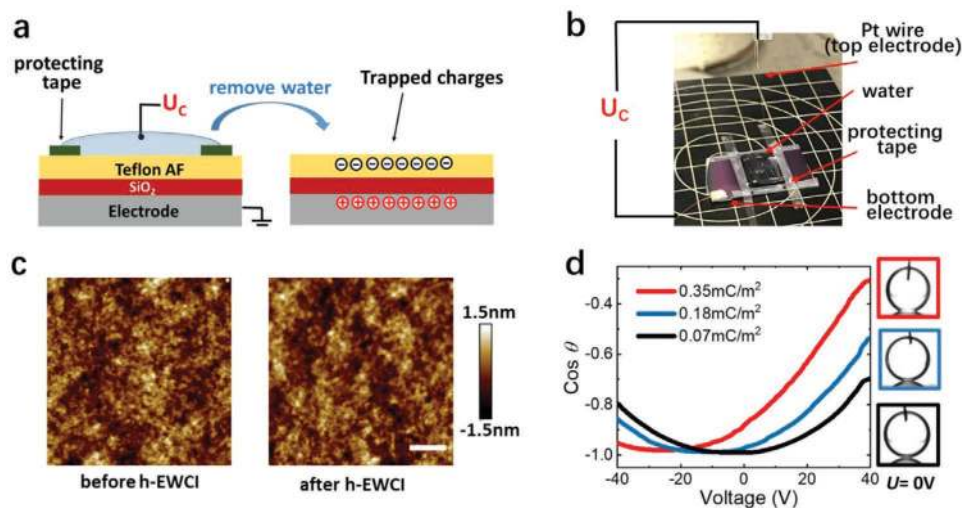

Figure 1. a) Schematic of the h-EWCI method. b) Picture of a sample being charged by using the h-EWCI method. The doped silica substrate served as the bottom electrode. The composite dielectric layer consisted of 300 nm thick SiO$_2$ (bottom layer) and 1 μm Teflon AF1600 (top layer). c) AFM images showing the surface topographies of Teflon AF1600 before and after h-EWCI process. Scale bar: 200 nm. d) Surface charge density versus applied voltage measured by the electrowetting probe. The trapping voltages U_T are −24 V for red, −12 V for blue and −5 V for black curves. The charging voltage U_c are −400 V for red, −300 V for blue and −200 V for blue curves. The charging time t_c are 15 min for all three samples. Snapshots show water drops at 0 V on the surfaces with σ of 0.35 mC m^{-2} for red, 0.18 mC m^{-2} for blue, and 0.07 mC m^{-2} for black curves.
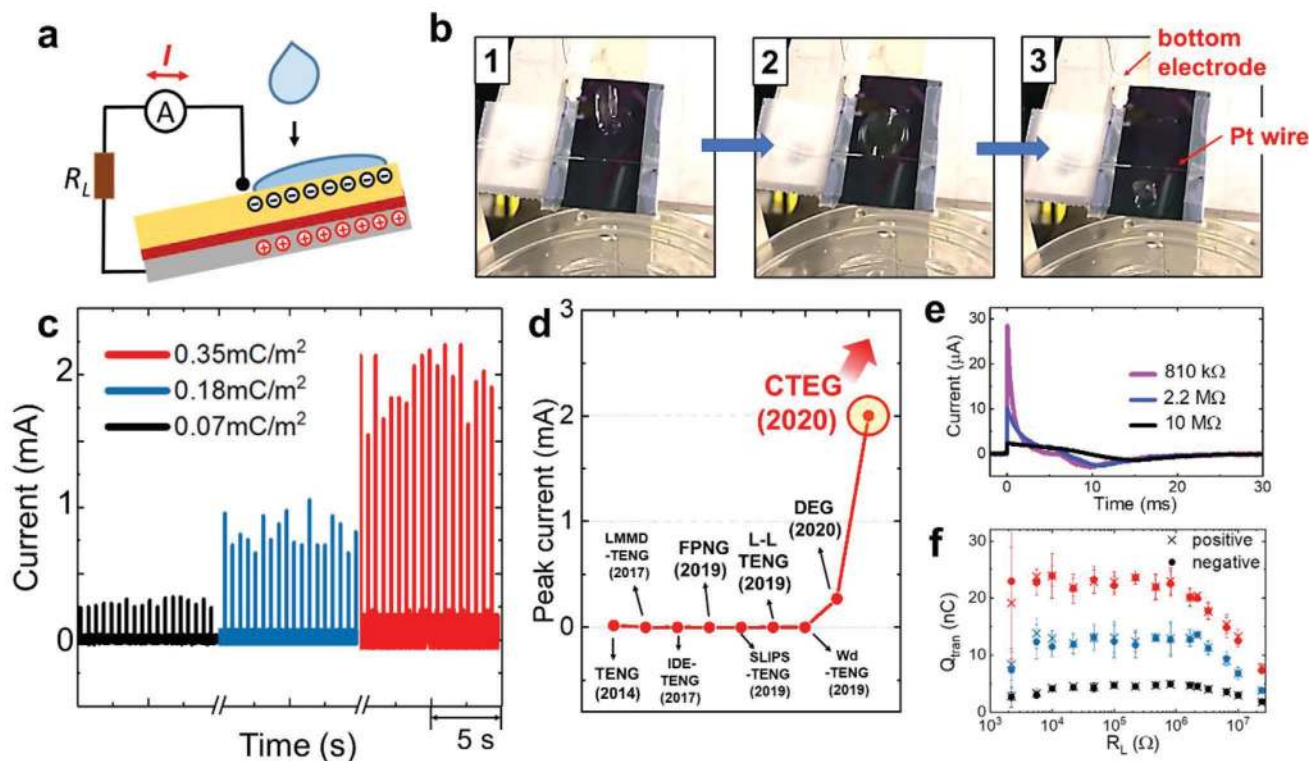
Figure 2. a) Schematic and b) snapshot of energy harvesting process in CTEG. In (a), orange layer: fluoropolymer; red layer: SiO_2; grey layer: bottom electrode (doped Si wafer). In (b), the pictures 1, 2, and 3 are the droplet falling on the surface, impacting and spreading on the surface, and sliding down on the surface, respectively. c) Generated current by multiple falling droplets with R_L of 2.2 kΩ. d) Comparison of the instantaneous peak current value obtained in this work with other reports.[4,27–32] e) Generated current by single falling droplet with different R_L. f) Total transferred charges varying with R_L at different surface charge densities (0.35 mC m^{-2} for red, 0.18 mC m^{-2} for blue, and 0.07 mC m^{-2} for black symbols). Positive and negative represent the current directions from the bottom to top electrodes and from the top to bottom electrodes, respectively.

as 0.35 mC m^{-2} could be achieved on a substrate with 300 nm thick SiO_2 layer and a 1 µm thick Teflon top layer (c = 14.8 µF).

After charging the surface, we mount a Pt wire on the top of the substrate as the top electrode, connect it to the bottom electrode via a load resistor R_L, and let the water droplets fall onto the pre-charged surface. The schematic and the photoshoots during drop impact are shown in **Figure 2**a,b; see supporting information for corresponding video sequences. The droplets first impact and then spread on the FP surface. When the drop reaches maximum spreading and touches Pt wire, a current peak is generated. Figure 2c shows such current peaks generated by multiple falling droplets with a load resistance R_L = 2.2 kΩ. The current peak value is proportional to the surface charge density.[26] Instantaneous current peaks higher than 2 mA can be generated by a droplet falling on a charged surface with σ = 0.35 mC m^{-2} (Figure 2c). This current value is substantially higher than previous reported values,[4,27–32] including the recent DEG approach[9] (Figure 2d; Table S1, Supporting Information). The current response is based on electrostatic induction and can be understood as follows: 1) before a droplet touches the wire, all countercharges induced by the trapped charges are located at the bottom electrode; 2) upon the spreading droplet touches the wire, the countercharges transfer from the bottom electrode to the top electrode, and an electric current signal is generated; 3) after the droplet bouncing

off or sliding downhill, the countercharges are again accumulated at the bottom electrode, ready for electricity generation from the next droplet. This process is illustrated in Figure S2 in the Supporting Information. The current peak I_0 generated by individual droplets decreases with increasing load resistance (R_L). Figure S3 in the Supporting Information shows the generated current peaks with a load resistance R_L = 6.5 MΩ, which are lower than those with R_L = 2.2 kΩ. Upon increasing R_L, the charge transfer in the circuit is increasingly hindered by R_L. Consequently, the charge transfer process is slowed down at a high R_L, and the generated current is thus lower than that with low R_L, as shown in Figure 2e. Given the initial surface potential on the fluoropolymer coating is U_T, the instantaneous current I_0 can be calculated as $I_0 = \frac{-U_T}{R_L} = \frac{\sigma}{R_L c}$. R_L and c are known parameters, so the charge density can be calculated from the I_0 as

$$\sigma = I_0 R_L c \tag{1}$$

We note that I_0 is indeed inversely proportional to R_L and the calculated σ based on this method, and is consistent with the σ_T measured by the EW probe (Figure S4, Supporting Information). Figure 2f shows the total transferred charges (Q_{tran}) as obtained by integrating the current for variable R_L. For a water droplet with a volume of 33 µL released from a
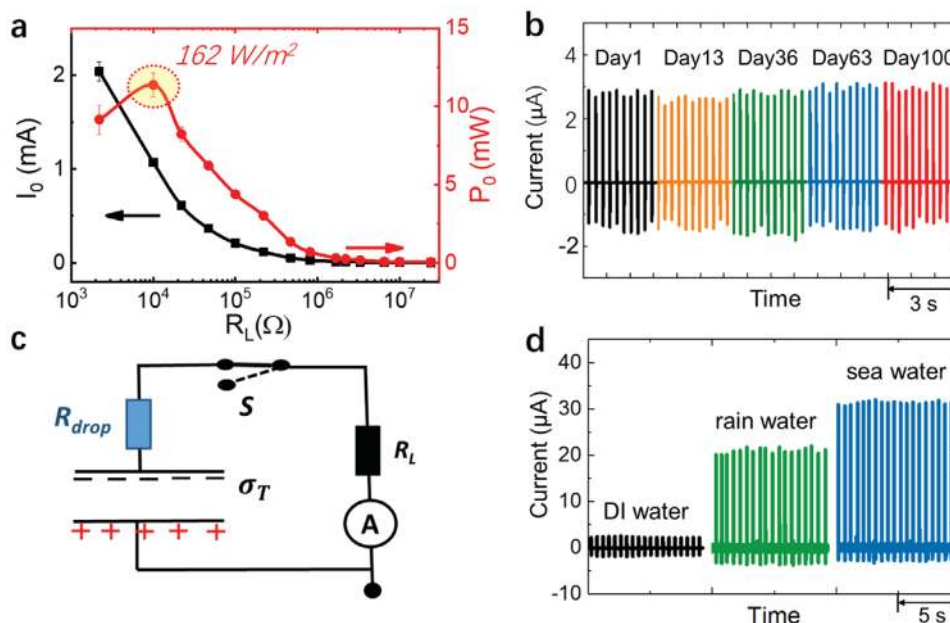
**ADVANCED
SCIENCE NEWS**
www.advancedsciencenews.com

**ADVANCED
MATERIALS**
www.advmat.de

Figure 3. a) Peak current (I_0) and power (P_0) as a function of loading resistance. (charging conditions: $U_T = -400$ V, $t = 15$ min; $\sigma = 0.35$ mC m^{-2}). b) Reliability test: the current generated from multiple falling droplets measured intermittently in 100 days (charging conditions: $U_T = -400$ V, $t = 5$ min; $R_L = 6.5$ MΩ, $\sigma = 0.27$ mC m^{-2}). c) Circuit diagram of CTEG. (R_L: load resistance; R_{drop}: resistance from the water droplet; "-" sign stands for negative charges; "+" sign represents positive charges; S is a switch, which stands for two states: when the droplet touches the Pt wire, the switch is on; when the droplet detaches the wire, the switch is off). d) Generated current using CTEG with droplets of DI water, rainwater and sea water. The droplet volume is 33 µL and the trapped charge density was 0.35 mC m^{-2}. All sample films prepared for measurements in this figure consisted of 300 nm SiO$_2$ as the bottom layer and 1 µm Teflon as the top layer.

height of 4.3 cm, the maximum spreading area is around 0.7 cm^2. The maximum transferred charge densities according to Figure 2f are 0.34, 0.19, and 0.07 mC m^{-2} for these three samples. These values are also consistent with the σ_T measured by the EW probe, demonstrating that the complete surface charge is indeed transferred through R_L in the external energy harvesting circuit. Note that there is no appreciable difference for energy harvested from an individual drop as compared to a train of consecutively impacting drops, Figure S5 (Supporting Information).

For the sample with surface charge density of 0.35 mC m^2, a maximum instantaneous power of 11.4 mW can be achieved by a single falling droplet, corresponding to a power density of 162 W m^{-2}. This is much higher than the power density of the conventional TENG, and also more than 3 times as high as that of the recently reported DEG.[9] The total energy harvested from a single drop is 0.35 µJ (Figure S6, Supporting Information). Taking into account the droplet's mechanical energy $E_{drop} = mgh = 14.2$ µJ (where $m = 33$ mg is the mass of the droplet, g is the gravitational acceleration and h = 4.3 cm is the height of the droplet), the energy harvesting efficiency can be calculated as $\eta = E/E_{drop}$. The maximum η around 2.5% has been achieved using such a substrate with $\sigma = 0.35$ mC m^{-2}. Moreover, according to the excellent stability of the surface charge densities generated by EWCI method,[17] the CTEG with the sample charged by h-EWCI showed excellent stability. We tested a CTEG device at intermittent time intervals throughout 100 days and did not detect any sign of degradation, **Figure 3**b. We tentatively attribute the enhanced stability to a field-induced injection of negative charge carriers into trapping

sides inside the FP material (Figure S7, Supporting Information) rather than residing exclusively at the surface. Such trapped charge carriers are protected and do not get exposed to the impinging water drops during operation. Therefore, they are more stable than the other types of surface charges. Since the low stability of surface charges generated by tribo-electrification is a congenital problem for the nanogenerators, such a long-term reliability is unique for any nanogenerator reported thus far.

To demonstrate the performance of the CTEG device, we tested it using droplets of DI water, rainwater (from Enschede in the Netherlands) and sea water (0.6 M NaCl solution), and the generated current are shown in Figure 3d. In contrast to other nanogenerators, including TENGs and DEGs, that display decreasing current signals with the increasing droplet conductivity, our CTEG device shows the opposite behavior, namely, the generated electricity increases with the droplet conductivity. This reversal of efficiency indicates that the mechanism of CTEG is different from other nanogenerators reported so far. It also implies that—unlike TENG and DEG—CTEG is also suitable for harvesting energy from drops of salty (sea) water. The physical reason for the decreased efficiency at low conductivity is CTEG is an increased resistance of the drop R_{drop} in the circuit (Figure 3c). The lower the droplet conductivity, the higher R_{drop} is. Consequently, I_0 can be calculated by $I_0 = \dfrac{-U_T}{R_L + R_{drop}}$, which increases with increasing of droplet conductivity. The observed order of peak currents is consistent with the measured conductivities of DI water, rain water and sea water of 0.038 µS cm^{-1}, 33.0 µS cm^{-1}, and 67.2 mS cm^{-1}.
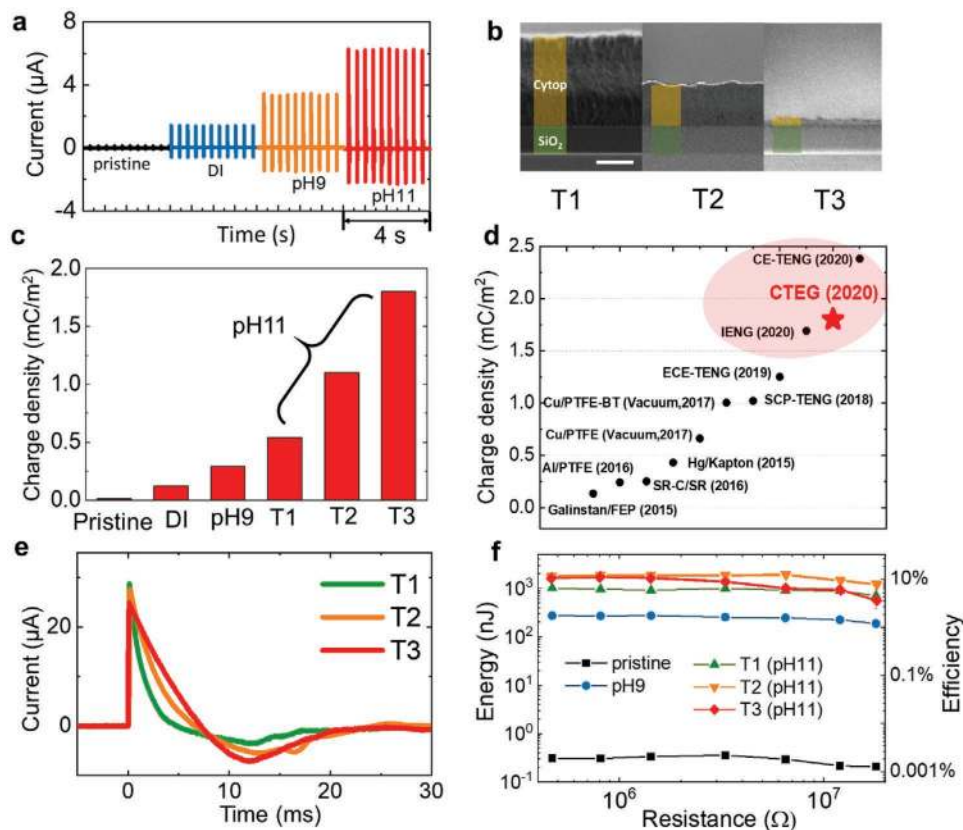
Figure 4. a) Output current of CTEG using the samples charged by aqueous solution at different pH. The dielectric stacks of the samples contain 400 nm thick SiO_2 as the bottom layer and 1.2 µm Cytop coating as the top layer. b) SEM images of the cross sections of samples T1, T2, and T3. (scale bar: 500 nm) c) Charge density generated from samples charged using h-EWCI at $U_c = -400$ V for 15 min. d) Comparison of the surface charge density obtained in this work with other reports.[11,15,36–42] e) Current generated from single falling droplet using CTEG with samples T1, T2, and T3. The loading resistance is 1.45 MΩ. f) Averaged harvested energy and energy conversion efficiency from 33 µL droplets falling from 5 cm height, as a function of loading resistance. The "pristine" means the original sample untreated by h-EWCI. The "pristine" means the original sample untreated by h-EWCI.

To further enhance the energy harvesting efficiency, we optimized the charging conditions of the h-EWCI process and the SiO_2-fluoropolymer dielectric stacks used in CTEG. As reported before, negative charges preferentially adsorbed at hydrophobic surfaces.[33–35] Previous observations indicated that fluoropolymer materials even spontaneously and permanently adsorb negative charges upon extended contact with water.[25] The highest charge densities had been reported for elevated pH. Therefore, we assume that electrolyte solutions with high pH will also enhance the trapped charge density in our h-EWCI process. By using a NaOH solution with pH = 11 during charging at our standard conditions ($U_c = -400$ V; charging time: 15 min), we indeed achieved a surface charge density of 0.54 mC m^{-2} on a composite dielectric layer with 400 nm thick SiO_2 and 1.2 µm Cytop 809M (Cytop). Lower charge densities but the same pH dependence was found for $U_c = -300$ V (Figure S8, Supporting Information). (Interestingly, this enhancement of σ at elevated pH was only found for Cytop but not for Teflon AF 1600 from Chemours Company, Figure S9 (Supporting Information). This different response may point to a role of different oxygen-containing polar co-monomers in the two FP materials for the trapping of negative charges.)

Since the σ generated by the EWCI method increased when applying higher electric fields during charging,[17] we varied

the thickness of the Cytop to achieve higher electric fields for charge injection[23] (Figure S10, Supporting Information). Three samples with the dielectric films composed of 400 nm thick SiO_2 layers that enhance the dielectric stability of the overall structure coated with various thicknesses of Cytop were prepared, being of 1.2 µm for sample T1, 500 nm for sample T2, and 120 nm for sample T3. **Figure 4**b shows the electron microscopy cross-sectional view of these three samples.

Measuring the peak current I_0 as a function of R_0 (Figure S11, Supporting Information) we extracted effective surface charge density σ of 0.56 ± 0.05, 1.15 ± 0.15, and 1.80 ± 0.25 mC m^{-2} for the samples T1, T2, and T3 (Figure 4c). The surface charge density value obtained by h-EWCI method has exceeded all the previous reports[11,15,36–40] except for the very recently proposed CE-TENG[41] (charge-excitation triboelectric nanogenerators) approach, as shown in Figure 4d and Table S2 (Supporting Information). Compared to the CE-TENG, h-EWCI has the advantage that the generated charge density is highly stable and does not need any further charge excitation processes during the operation of the nanogenerators. The current generated from individual falling droplets on these three samples ($R_L = 1.45$ MΩ) is shown in Figure 4c. The current peaks are very similar because the effect of increasing σ for thinner samples is largely compensated by the increasing capacitance

**ADVANCED
SCIENCE NEWS**

www.advancedsciencenews.com

**ADVANCED
MATERIALS**

www.advmat.de

c (see Equation (1)). While the initial current values I_0 and U_T for these three samples were thus very similar, the width of the current curves with respect to time is increased with σ (Figure 4e). This indicates that the instantaneous current or voltage values were not the only parameters for characterizing and evaluating the electricity generation process of nanogenerators. By applying these samples into CTEGs, micro-joule level energy could be harvested from a 33 µL water droplet falling from a height of 5 cm. The harvested energy is calculated using $E = \int I^2 R_L dt$ from the current generated from single droplet. As shown in Figure 4f, for a pristine Cytop film without h-EWCI charging, the energy harvesting efficiency is much lower than from the films treated with h-EWCI. For the identical dielectric stacks of 400 nm thick SiO_2 and 1.2 µm thick Cytop, the higher σ results in higher energy harvesting efficiency. According to the samples with different dielectric layers, the harvested energy is not only determined by σ. For instance, η is very similar for samples T2 and T3 despite the fact that sample T3 displays a significantly higher surface charge density. We suppose that the thick dielectric layers help enhance the electric energy stored in the dielectric capacitors and thus more energy can be released when the droplet touches the top electrode. Using the sample treated by the optimized h-EWCI process, a maximum energy of 1.96 µJ can be harvested from single falling droplet (Figure 4f). Considering $E_{drop} = mgh = 16.5$ µJ (m = 33 mg, $h = 5$ cm), the energy harvesting efficiency reaches 11.8%, which is much higher than 0.01% achieved in TENG,[5] and 5.36 times of the most recently reported value of 2.2%.[9]

These results suggest that CTEG is indeed a viable energy harvesting method provided that a suitable intensive source of droplets is available. The reported harvested energy of ≈ 2 µJ per drop implies that the electrical energy required for the initial charging process of 20 mJ cm^{-2} can be recovered after 10 000 drop impacts. Given a response time of < 20 ms per drop (Figure 2d), the device can harvest this energy within less than 1/2 h. The fabrication of the substrates is based on standard fabrication processes from the semiconductor and display industries.[43] It is therefore highly parallel provided that the Pt wire in our experiments is replaced by deposited or printed electrodes on the substrate. Further optimization of the dielectric stack may lead to even further increases in efficiency.

In summary, we developed a novel electricity generator, Charge Trapping-based Electricity Generator (CTEG), based on the stably trapped charges on hydrophobic fluoropolymer surfaces. By utilizing CTEG, we could overcome important bottlenecks of conventional nanogenerators, namely the low power density, the low and unstable surface charges density along with poor long-term reliability. Instantaneous current higher than 2 mA and power density of 162 W m^{-2} have been achieved. Surface charge density as high as 1.8 mC m^{-2} allowed an ultrahigh energy harvesting efficiency of 11.8% from a falling water droplet. Moreover, the excellent reliability for 100 days' testing, as well as its applicability with highly conductive liquid suggest a promising future for industrialization of this invention. Therefore, our approach can also be considered for applications beyond drop-based energy harvesting, such as for energy harvesting from ocean waves, in wearable electricity generation devices, as well as various sensors.

Conflict of Interest

The authors declare no conflict of interest.

[1] T. Krupenkin, J. A. Taylor, *Nat. Commun.* **2011**, *2*, 448.
[2] H. Yang, S. Hong, B. Koo, D. Lee, Y.-B. Kim, *Nano Energy* **2017**, *31*, 450.
[3] Z. H. Lin, G. Cheng, L. Lin, S. Lee, Z. L. Wang, *Angew. Chem.* **2013**, *125*, 12777.
[4] G. Zhu, Y. Su, P. Bai, J. Chen, Q. Jing, W. Yang, Z. L. Wang, *ACS Nano* **2014**, *8*, 6031.
[5] Z. H. Lin, G. Cheng, S. Lee, K. C. Pradel, Z. L. Wang, *Adv. Mater.* **2014**, *26*, 4690.
[6] S. S. Kwak, S. Lin, J. H. Lee, H. Ryu, T. Y. Kim, H. Zhong, H. Chen, S.-W. Kim, *ACS Nano* **2016**, *10*, 7297.
[7] D. Yoo, S.-C. Park, S. Lee, J.-Y. Sim, I. Song, D. Choi, H. Lim, D. S. Kim, *Nano Energy* **2019**, *57*, 424.
[8] K. Tao, H. Yi, Y. Yang, H. Chang, J. Wu, L. Tang, Z. Yang, N. Wang, L. Hu, Y. Fu, *Nano Energy* **2019**, 104197.
[9] W. Xu, H. Zheng, Y. Liu, X. Zhou, C. Zhang, Y. Song, X. Deng, M. Leung, Z. Yang, R. X. Xu, *Nature* **2020**, *578*, 392.
[10] H. Zou, Y. Zhang, L. Guo, P. Wang, X. He, G. Dai, H. Zheng, C. Chen, A. C. Wang, C. Xu, *Nat. Commun.* **2019**, *10*, 1427.
[11] W. Liu, Z. Wang, G. Wang, G. Liu, J. Chen, X. Pu, Y. Xi, X. Wang, H. Guo, C. Hu, *Nat. Commun.* **2019**, *10*, 1426.
[12] Z. H. Lin, G. Cheng, L. Lin, S. Lee, Z. L. Wang, *Angew. Chem., Int. Ed.* **2013**, *52*, 12545.
[13] F.-R. Fan, Z.-Q. Tian, Z. L. Wang, *Nano Energy* **2012**, *1*, 328.
[14] K. Zhao, X. Wang, Y. Yang, *Adv. Mater. Technol.* **2017**, *2*, 1600233.
[15] L. Xu, T. Z. Bu, X. D. Yang, C. Zhang, Z. L. Wang, *Nano Energy* **2018**, *49*, 625.
[16] H. Wu, F. Mugele, G. Zhou, *China Patent CN110665552A*, **2019**.

**ADVANCED
SCIENCE NEWS**

www.advancedsciencenews.com

**ADVANCED
MATERIALS**

www.advmat.de

[17] H. Wu, R. Dey, I. Siretanu, D. van den Ende, L. Shui, G. Zhou, F. Mugele, *Small* **2020**, *16*, 1905726.

[18] G. Zhou, H. Wu, F. Mugele, *China Patent CN110572071A*, **2019**.

[19] H. Wu, L. Shui, F. Li, R. Hayes, A. Henzen, F. Mugele, G. Zhou, *ACS Appl. Nano Mater.* **2019**, *2*, 1018.

[20] E. Seyrat, R. A. Hayes, *J. Appl. Phys.* **2001**, *90*, 1383.

[21] R. Zhou, S. Fu, H. Jiang, X. Li, G. Zhou, *Results Phys.* **2019**, *15*, 102737.

[22] H. Wu, H. Li, A. Umar, Y. Wang, G. Zhou, *Materials* **2018**, *11*, 2474.

[23] E. Harari, *J. Appl. Phys.* **1978**, *49*, 2478.

[24] J. Buehrle, S. Herminghaus, F. Mugele, *Phys. Rev. Lett.* **2003**, *91*, 086101.

[25] A. G. Banpurkar, Y. Sawane, S. M. Wadhai, C. Murade, I. Siretanu, D. van den Ende, F. Mugele, *Faraday Discuss.* **2017**, *199*, 29.

[26] H. Wu, N. Mendel, D. van den Ende, G. Zhou, F. Mugele, in *arXiv e-prints*, **2020**, arXiv:2001.05019.

[27] B. K. Yun, H. S. Kim, Y. J. Ko, G. Murillo, J. H. Jung, *Nano Energy* **2017**, *36*, 233.

[28] B. Zhang, L. Zhang, W. Deng, L. Jin, F. Chun, H. Pan, B. Gu, H. Zhang, Z. Lv, W. Yang, *ACS Nano* **2017**, *11*, 7440.

[29] Y. Lu, H. Wu, Q. Yang, J. Ping, J. Wu, J. Liu, *Adv. Sustainable Syst.* **2019**, *3*, 1900012.

[30] J. H. Lee, S. Kim, T. Y. Kim, U. Khan, S.-W. Kim, *Nano Energy* **2019**, *58*, 579.

[31] W. Xu, X. Zhou, C. Hao, H. Zheng, Y. Liu, X. Yan, Z. Yang, M. Leung, X. C. Zeng, R. X. Xu, *Nat. Sci. Rev.* **2019**, *6*, 540.

[32] J. Nie, Z. Wang, Z. Ren, S. Li, X. Chen, Z. L. Wang, *Nat. Commun.* **2019**, *10*, 2264.

[33] A. Z. Stetten, D. S. Golovko, S. A. Weber, H.-J. Butt, *Soft Matter* **2019**, *15*, 8667.

[34] T. Preočanin, A. Selmani, P. Lindqvist-Reis, F. Heberling, N. Kallay, J. Lützenkirchen, *Colloids Surf. A* **2012**, *412*, 120.

[35] R. Zimmermann, U. Freudenberg, R. Schweiß, D. Küttner, C. Werner, *Curr. Opin. Colloid Interface Sci.* **2010**, *15*, 196.

[36] W. Tang, T. Jiang, F. R. Fan, A. F. Yu, C. Zhang, X. Cao, Z. L. Wang, *Adv. Funct. Mater.* **2015**, *25*, 3718.

[37] Y. Zi, S. Niu, J. Wang, Z. Wen, W. Tang, Z. L. Wang, *Nat. Commun.* **2015**, *6*, 8376.

[38] T. Zhou, L. Zhang, F. Xue, W. Tang, C. Zhang, Z. L. Wang, *Nano Res.* **2016**, *9*, 1442.

[39] J. Wang, S. Li, F. Yi, Y. Zi, J. Lin, X. Wang, Y. Xu, Z. L. Wang, *Nat. Commun.* **2016**, *7*, 12744.

[40] J. Wang, C. Wu, Y. Dai, Z. Zhao, A. Wang, T. Zhang, Z. L. Wang, *Nat. Commun.* **2017**, *8*, 88.

[41] Y. Liu, W. Liu, Z. Wang, W. He, Q. Tang, Y. Xi, X. Wang, H. Guo, C. Hu, *Nat. Commun.* **2020**, *11*, 1599.

[42] L. Gu, J. Liu, N. Cui, Q. Xu, T. Du, L. Zhang, Z. Wang, C. Long, Y. Qin, *Nat. Commun.* **2020**, *11*, 1030.

[43] H. Wu, B. Tang, R. A. Hayes, Y. Dou, Y. Guo, H. Jiang, G. Zhou, *Materials* **2016**, *9*, 707.

2001699 (7 of 7)